RNA (1997), 3:602–612. Cambridge University Press. Printed in the USA.

Exact determination of UV-induced crosslinks in 16S ribosomal RNA in 30S ribosomal subunits

CHRISTOPHER WILMS,[1]* JAMES W. NOAH,[1]* DEGANG ZHONG,[2,3] and PAUL WOLLENZIEN[1]

[1] Department of Biochemistry, North Carolina State University, Raleigh, North Carolina 27695-7622, USA
[2] E.A. Doisy Department of Biochemistry and Molecular Biology, St. Louis University Medical Center, St. Louis, Missouri 63104, USA

ABSTRACT

***Escherichia coli* 30S ribosomal subunits were UV-irradiated to induce intramolecular crosslinks in the 16S rRNA. Intact 16S rRNA was purified and subjected to gel electrophoresis, under denaturing conditions, to separate molecules on the basis of the crosslinked loop size. Molecules separated this way were enriched for specific crosslinks and could be analyzed by the reverse transcription arrest assay to determine exact crosslinking sites. Thirteen crosslinking sites have been identified at single nucleotide resolution. Of these, eight are within or adjacent to secondary structure elements: one of these (C582 × G760) involves an interaction between nucleotides within an interior loop, one (C1402 × X1501) involves an interaction between nucleosides in adjacent base pairs, and the others involve interactions between nucleotides that are within junction regions (A441 × G494, U562 × U884, C934 × U1345, and U991 × U1212) or are interactions between nucleotides (C54 × A353 and U1052 × C1200) that somehow cross known base pairs. Five other crosslinks connect sites distant in the secondary structure and provide global constraints for the arrangement of RNA regions within RNA domains I and II (U244 × G894, G894 × A1468, C967 × C1400) and within domain III (U1126 × C1281 and A1093 × G1182). These crosslinks, known at single-nucleotide resolution, are useful in the prediction of local RNA regions, as well as the global structure.**

Keywords: intramolecular RNA–RNA crosslinks; molecular modeling; reverse transcription arrest assay; 16S rRNA three-dimensional structure

INTRODUCTION

The secondary structures of the ribosomal RNAs have been determined, to a large extent, by finding covariance of nucleotides as a proof of base–base interaction (Gutell et al., 1994). For the 16S-like rRNAs, there are now approximately 70 regions of complementary sequences within the molecule. Several of these occur as long-range interactions in the center of the rRNA molecule, which would be otherwise difficult to predict from thermodynamic considerations (Konings & Gutell, 1995). In addition, there are examples of base covariance that suggest other types of long-range or tertiary interactions; these include three cases of nucleotide–nucleotide interactions that are part of pseudo-knot structures, many examples of noncanonical nucleotide–nucleotide interaction, and several other areas in which there are single, stand-alone nucleotide pair interactions. To date, these comparisons have not yielded the same density of co-variances between nucleotides distant in the secondary structure as those found in tRNA (Levitt, 1969; Quigley & Rich, 1976; Sussman & Kim, 1976) or in the core structure of the group I introns (Michel & Westhof, 1990), so they do not yet allow the prediction of a compact three-dimensional structure. Additional information for the overall folding of the 16S rRNA might be obtained by RNA crosslinking experiments that could indicate additional long-range interactions not already known from sequence comparison. In addition, crosslinking experiments, or other types of distance detection experiments, ultimately may be needed to determine the extent of conformational flexibility in the subunits and the nature of the structural changes that occur in the rRNAs during their function.

UV irradiation is able to activate the joining of nucleotide units in RNA if they are within a short distance and occur, at least transiently, in the correct geometry (Zwieb & Brimacombe, 1980; Atmadja & Bri-

Reprint requests to: Paul Wollenzien, Department of Biochemistry, Box 7622, North Carolina State University, Raleigh, North Carolina 27695-7622, USA; e-mail: wollenz@bchserver.bch.ncsu.edu.

*The first two authors contributed equally to the work.

[3]Present address: American Red Cross, Holland Laboratory, 15601 Crabbs Branch Way, Rockville, Maryland 20855, USA.

macombe, 1985; Stiege et al., 1986; Budowsky & Abdurashidova, 1989). UV crosslinking has the advantage that native ribosomal particles can be examined without the necessity of introducing extrinsic probes, and it is even possible to perform UV crosslinking in vivo (Stiege et al., 1988). So far, this method has been used to determine 16 crosslinks in the *Escherichia coli* 16S rRNA, although only a part of these have been reported at single-nucleotide resolution. Ten of these were within or adjacent to secondary structure interactions, and were designated secondary structure crosslinks, six were between nucleotides not close in the secondary structure and were designated as tertiary structure crosslinks (Atmadja & Brimacombe, 1985). The determination of the crosslinks in 16S rRNA has been made by methods that fragment the crosslinked rRNA so that searches could be made for fragments containing crosslinks by electrophoresis methods (Zwieb et al., 1978; Zwieb & Brimacombe, 1980; Thompson & Hearst, 1983; Stade et al., 1989) and hybridization methods (Stiege et al., 1988). Because of the initial fragmentation of the RNA, crosslinking sites were determined by RNA fingerprinting, and this did not always yield exact sites. Hence, the crosslinking sites were specified as occurring between sequence intervals.

An alternative method is used in this report for crosslink identification and site determination. Intact full-length 16S rRNA is purified after UV irradiation and then is separated by electrophoresis on the basis of the covalent crosslinked loops contained in some of the molecules. Separated crosslinked molecules are then analyzed by primer extension experiments that depend on the arrest of reverse transcriptase at the site of the UV crosslink (Denman et al., 1988; Cunningham et al., 1992). These types of methods already have been used for the analysis of crosslinks in molecules of shorter size than 16S rRNA (Teare & Wollenzien, 1989, 1990; Lemaigre-Dubreuil et al., 1991; Harris et al., 1994; Weeks & Cech, 1995). Thirteen crosslinks in 16S rRNA determined by this approach are described here. Seven of these confirm, at higher resolution, crosslinks that were reported previously (Zwieb & Brimacombe, 1980; Atmadja & Brimacombe, 1985; Stiege et al., 1986, 1988), and six are new. The significance of the crosslinks with respect to the 16S rRNA three-dimensional structure and its modeling are discussed.

RESULTS

Time courses of UV crosslinking and tRNA binding activity

30S subunits were irradiated for 10, 30, 60, and 80 min, and 16S rRNA was purified by proteinase digestion, phenol extraction, and electrophoresis on agarose gels and was then 5′-[^{32}P]-end-labeled. Samples of these RNAs and an nonirradiated control 16S rRNA were examined by electrophoresis on denaturing, low-concentration polyacrylamide gels. Under these conditions, RNA molecules separate on the basis of the size of the covalent loops they contain (Teare & Wollenzien, 1989, 1990; Lemaigre-Dubreuil et al., 1991). The samples showed patterns of bands attributed to crosslinking, with increasing intensity of the bands as a function of time of irradiation (Fig. 1). Measurements of the sum of intensity of the crosslinked bands show their frequency asymptotically approaches a maximum. The sum of the crosslinked RNA after 10 min was about 12%; after 30 min, 19%; after 60 min, 25%; and after 80 min, 28%. This type of behavior is characteristic of UV-induced crosslinking (Budowsky & Abdurashidova, 1989). The ability of the 30S subunits to bind tRNA after increasing exposure to UV irradiation was tested by determining tRNA-binding ability using the filter binding assay (Nirenberg & Leder, 1964). Scatchard plots of binding data indicate one strong binding site (data not shown) that should correspond to the P site (Makarov et al., 1985). There is a gradual de-

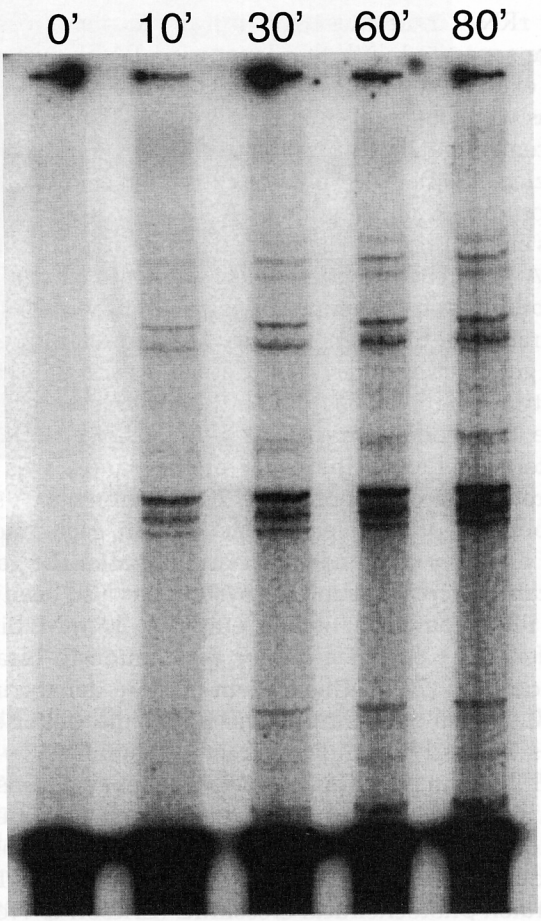

FIGURE 1. Dependence of crosslinking on length of irradiation. 30S subunits were irradiated for the indicated times and RNA was extracted, purified on agarose gels, and 5′ end-labeled. Electrophoresis was on 3.6% polyacrylamide/8.3 M urea gels in TBE buffer. Linear control 16S rRNA is contained in the heavy band close to the bottom of the figure in this view.

crease in the stoichiometry of tRNA binding from 0.9 to 0.75 for subunits irradiated from 0 to 80 min, and a gradual decrease in the association constant from 4.7×10^7 M to 4.3×10^7 M for subunits irradiated from 0 to 60 min, and then a more substantial decrease to 3.0×10^7 M for subunits irradiated for 80 min. A crosslinking time of 20 min was picked as a standard time because this generated a reasonable frequency of crosslinked molecules before a significant amount of inactivation occurred. Twenty-minute irradiation corresponds to a dose of approximately 5 photons per nucleotide given the measured intensity of the light (1.6 mwatts/cm^2) and its wavelength (nominally 300 nm) and the absorbance of the sample. UV irradiation should induce RNA–protein crosslinks such as the crosslinking of nt 1239 to protein S7 (Zwieb & Brimacombe, 1979); these are either at low levels under our conditions or are not detectable by primer extension experiments after proteinase K treatment.

Determination and assignment of UV crosslinking sites

16S rRNA molecules with intramolecular crosslinks were separated with the denaturing PAGE system. In the example of the experiments shown here, 18 fractions were cut from the gel and the RNA was purified by centrifugation through CsCl solution (Wilms & Wollenzien, 1994). After phenol extraction and reprecipitation, an equal amount of RNA from each fraction was electrophoresed again under the same conditions. RNA from each fraction electrophoresed at the same mobility as on the preparative gel, and there was little degradation of the RNA (Fig. 2), demonstrating that the gel electrophoresis reproducibly separates different types of molecules. Under the conditions described here, the general appearance of the gel electrophoretic pattern, including the order of the bands, was very reproducible over more than 20 experiments. A small amount of photoreversal was seen in each fraction; this probably occurs during handling after the gel purification step. A second gel system has also been used for this separation, which employs 30 mM Bis-tris buffer, pH 6.8, and a higher acrylamide to bisacrylamide ratio (70:1). This system is more denaturing at 45 °C, is less damaging to the RNA, and better separates molecules with lower relative mobility.

All fractions were analyzed by the reverse transcription arrest assay using AMV reverse transcriptase. For cyclobutane-type UV crosslinks between pyrimidine residues (Denman et al., 1989; Cunningham et al., 1992), psoralen photochemical crosslinks (Ericson & Wollenzien, 1986), and photo-crosslinks produced by 4-thiouridine (Lemaigre-Dubreuil et al., 1991), AMV reverse transcriptase stops one nucleotide before the site of a crosslink, giving rise to a darker than normal primer extension step at that location. For the pyrimidine

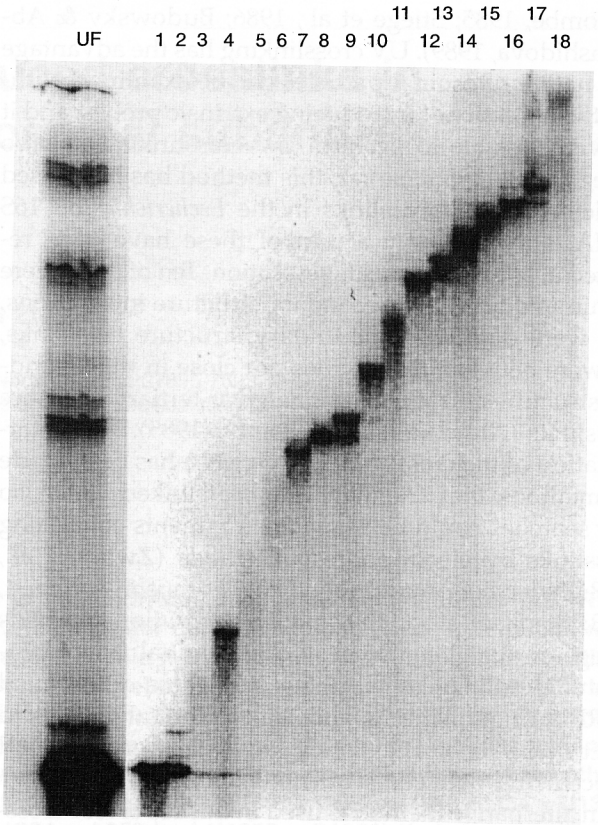

FIGURE 2. Separation of crosslinked RNA by gel electrophoresis. Crosslinked 16S rRNA (100 μg) was separated as described in Materials and Methods on a 3.6% polyacrylamide/8.3 M urea gel in TBE buffer; 18 regions were cut from the gel and RNA was eluted from them by centrifugation through cesium chloride cushion. A part of each of the fractions was re-electrophoresed in the same gel system as shown here. The double lane on the left contains part of the original unfractionated sample.

cyclobutane-type UV crosslinks and psoralen crosslinks, reverse transcriptase cannot proceed through the crosslinked site, but for the 4-thiouridine-induced crosslinks there is low efficiency read-through at some crosslinking sites (Lemaigre-Dubreuil et al., 1991). Therefore, at least two primers may be needed to determine both nucleotides involved in the crosslink: at least one primer to detect the participating 3′ nucleotide, and at least one primer for the participating 5′ nucleotide. Figure 3A shows a reverse transcription experiment with a primer complementary to the interval 1453–1469, close to the 3′ end of the 16S rRNA, and Figure 3B shows an experiment with a primer complementary to the interval 861–878. Usually 10 different DNA primers were used on all fractions, and all stopping points for reverse transcription were noted. Additional DNA primers were used to analyze RNA regions just to the 5′ side of some crosslinking sites. In some instances, more than two stopping points (apparent crosslinks) are seen in the RNA from a fraction. In these cases, a correlation between large loop size and slow gel electrophoretic mobility was used to help establish which reverse transcription sites belong together.

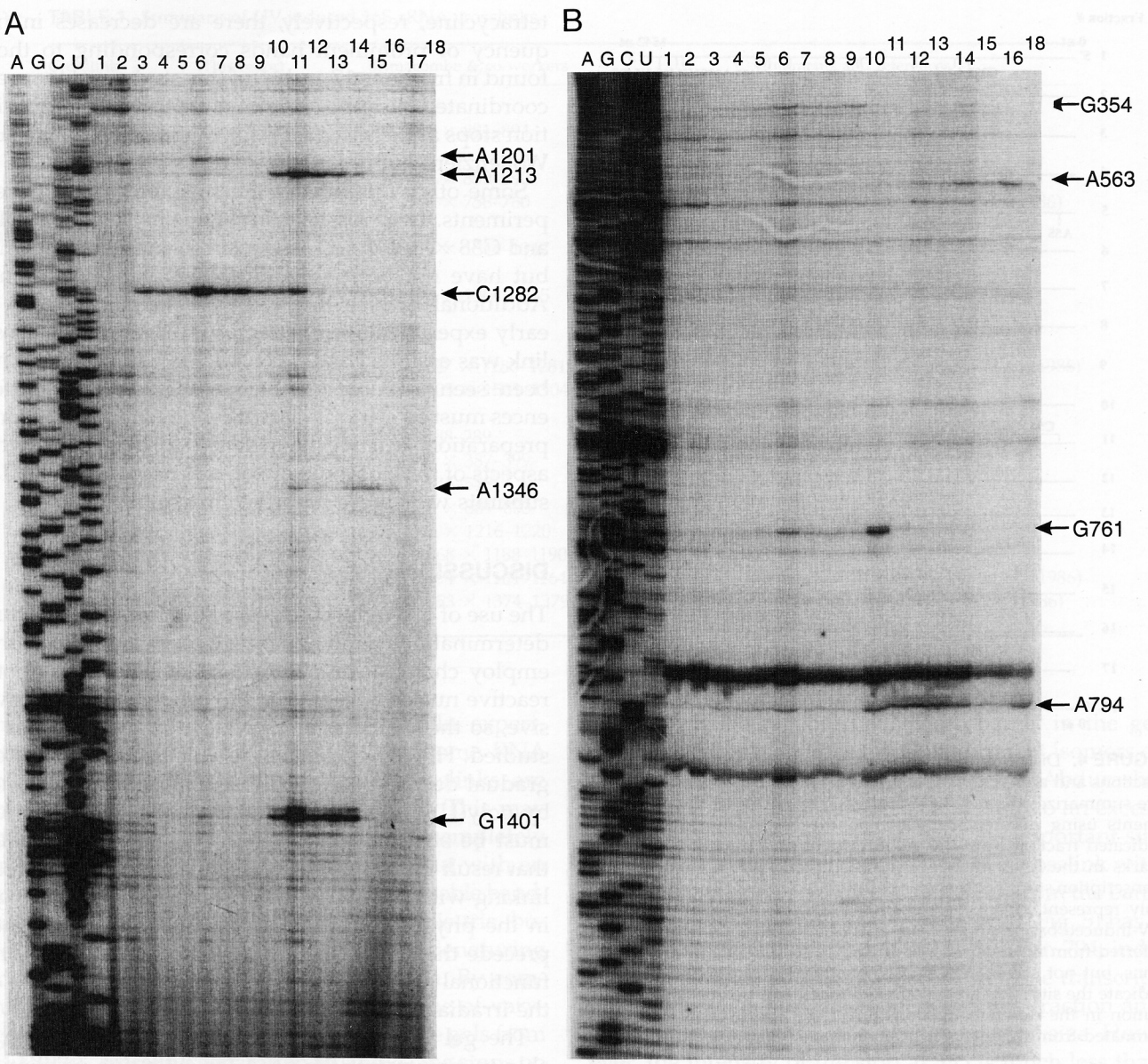

FIGURE 3. Reverse transcription arrest analysis of crosslinked 16S rRNA. Patterns of primer extension using DNA oligonucleotide primers complementary to 1453–1469 (**A**) and 861–878 (**B**) were determined by gel electrophoresis. A crosslink site usually is seen as a single, stronger-than-usual band, one nucleotide on the 3′ side of the actual crosslink, in one or a range of fractions. Lanes containing sequencing reactions and lanes containing primer extensions performed on RNA from the different fractions are indicated at the top. Identified crosslink sites are indicated on the right of each panel. Positions labeled in this figure are the reverse transcription stops.

Figure 4 shows a summary of the data obtained from the reverse transcription analysis of 18 fractions from a preparative gel; in this case, the separation was done in the gel system that used BTBE buffer. The locations of UV-modified nucleotides inferred from reverse transcription stops seen in every RNA fraction but not in nonirradiated RNA are indicated by tic marks in fraction 1; nucleotide positions for these types of sites are listed below the line for fraction 1. Crosslinking sites inferred from the pattern of reverse transcription stops in fractions 2–18 are shown by connecting lines. Additional sites detected by reverse transcription stops in fractions 2–18 that may be present because of crosslinking, but for which crosslink partners have not been identified, are shown by tic marks and are identified by nucleotide position.

Thirteen crosslinks found in these studies are summarized in Table 1. At all sites except four, reverse transcriptase stops at a single site and the nucleoside at the 5′ side of that site is taken as the crosslink. In the exceptions, two adjacent nucleosides are observed as stops and the 5′ one of these is taken as the crosslinking site (see Teare & Wollenzien, 1990; Cunningham et al., 1992). The reverse transcription analysis was

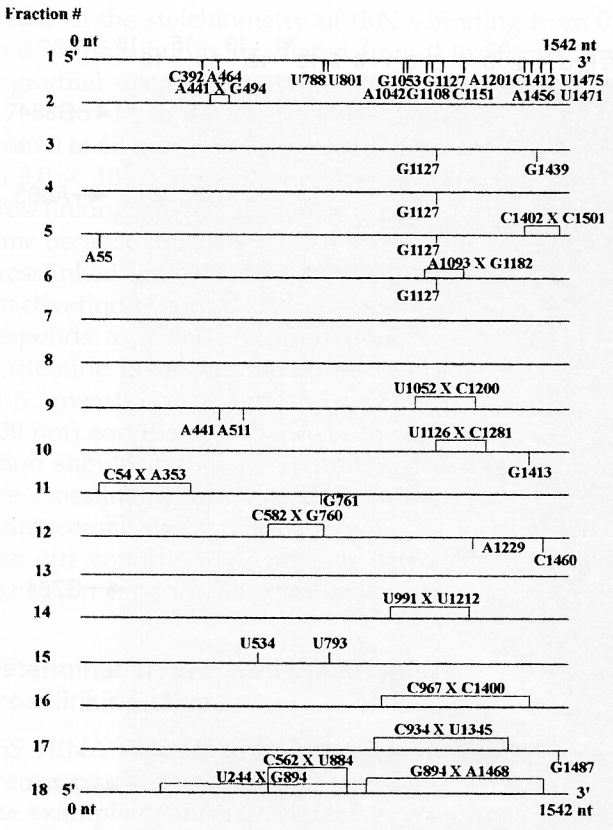

FIGURE 4. Distribution of UV-induced sites in RNA from different fractions and assignment of crosslinking sites. Each line in this figure summarizes the results of multiple reverse transcription experiments using different primers and the RNA isolated from the indicated fraction from the gel electrophoresis separation. The tic marks in the RNA fraction 1 indicate sites inferred from reverse transcription stops not seen in nonirradiated 16S rRNA and presumably represent local UV-induced base dimers and other types of UV-induced base changes. Tic marks in fractions 2–18 indicate sites inferred from reverse transcription stops seen in one or more fractions, but not seen in RNA from fraction 1. The connecting lines indicate the sites that are crosslinked together based on their distribution in the different fractions and their approximate loop size estimated from their gel electrophoretic mobility.

also performed after $NaBH_4$ reduction and aniline cleavage (Peattie, 1979) on fractions containing the crosslinks 244 × 894, 894 × 1468, and 1052 × 1200, and on fractions 2, 4, and 13 (in which crosslinks had not been found) to determine if there might be other types of UV-induced crosslinks present in these fractions that would not cause the stopping of reverse transcriptase, but might be cleavable and hence detectable after cleavage reactions. For the UV crosslinked samples, the same fraction-specific stopping points were seen without or with the reduction and cleavage steps; some additional stopping points were seen in all fractions and were attributed to crosslinks between adjacent nucleotides or reactions of the nucleotides with solvent (data not shown). The assignment of the crosslinks C934 × U1345 and U967 × C1400 have been confirmed in experiments that investigated the effects of antibiotics on the 30S ribosome. In the presence of spectinomycin or tetracycline, respectively, there are decreases in frequency of prominent bands corresponding to those found in fractions 17 and 16 of this study, and there are coordinated disappearances in the reverse transcription stops at the assigned pairs of sites (J.W. Noah & P. Wollenzien, unpubl. data).

Some other crosslinks were seen, but not in all experiments. Two crosslinks involving nt 38 (G38 × G402 and G38 × A397) were detected in early experiments, but have not been seen in subsequent experiments. Additional reverse transcription stops were seen in early experiments in the region 1120–1180; one crosslink was assigned as C1109 × U1189, but this has not been seen in subsequent experiments. These differences must be attributed to differences in the ribosome preparation, but we have failed to determine what aspects of the ribosome or subunit preparation lead to subunits with these different structural features.

DISCUSSION

The use of UV-induced crosslinking for RNA structure determination has an advantage over experiments that employ chemical or photochemical agents or photoreactive nucleosides in that the procedure is noninvasive, so the structure of native active subunits can be studied. However, exposure to UV light does cause a gradual decrease in functional activity as determined by poly(U)-directed tRNA binding. In addition, there must be structural changes in the subunits, as well, that result in the nonlinear response in extent of crosslinking with time. The data indicate that the changes in the physical structure of the subunit significantly precede the loss of tRNA binding activity. Additional functional activities have not been determined yet on the irradiated 30S subunits.

The gel electrophoresis method employed here is able to circumvent the need for extensive irradiation because the crosslinked RNA species can be enriched greatly before primer extension analysis. The present gel electrophoresis conditions are 3.6% polyacrylamide at 40:1 acrylamide:bisacrylamide with 8.3 M urea in TBE buffer or, alternatively, 3.6% polyacrylamide at 70:1 acrylamide:bisacrylamide with 8.3 M urea and BTBE buffer. Larger amounts of 16S rRNA can be separated on these gel systems than on polyacrylamide gels made with formamide (Ericson & Wollenzien, 1988; Wollenzien, 1988) and the gels are more reproducible. Molecules with crosslinks in the size range 50 nt to about 700 nt are separated in the present gel system; molecules with crosslink sizes smaller than this are not separated from the parent linear 16S rRNA, and the ability to separate different crosslinked molecules from one another is lost at larger crosslink sizes. The separation of molecules with long-range crosslinks is an advantage because these are more likely to provide important information pertaining to the global three-

TABLE 1. Summary of UV-induced 16S rRNA crosslinks.

Crosslink	This report	Brimacombe & co-workers	Comments and references
1	C54 × A353		2°
2	U244 × G894	243–244 × 891–894	3° Stiege et al. (1988)
3	A441 × G494		2°
4	U562 × U884	559–566 × 850–890	2° Stiege et al. (1988)
5	C582 × G760	582–584 × 756–760	2° Zwieb & Brimacombe (1980); Stiege et al. (1986)
6	G894 × A1468		3°
7	C934 × U1345	934–939 × 1344–1347	2° Stiege et al. (1988)
8	C967 × C1400		3°
9	U991 × U1212	989–993 × 1208–1215	2° Stiege et al. (1988)
10	A1093 × G1182		3°
11	U1052 × C1200		2°
12	U1126 × C1281	1125–1127 × 1280–1281	3° Atmadja & Brimacombe (1985); Stiege et al. (1986)
13	G1402 × A1501	1402–1405 × 1501–1504	2° Doring et al. (1992)
14		31 × 48	3° Atmadja & Brimacombe (1985)
15		118 × 288–289	3° Stiege et al. (1986)
16		366–369 × 387–399	2° Stiege et al. (1986)
17		497 × 545–548	3° Atmadja & Brimacombe (1985)
18		779–785 × 801–803	2° Stiege et al. (1988)
19		977–987 × 1216–1220	2° Stiege et al. (1988)
20		1065–1068 × 1188–1190	2° Stiege et al. (1988)
21		1090–1094 × 1161–1164	3° Atmadja & Brimacombe (1985); Stiege et al. (1986)
22		1348–1353 × 1374–1379	2° Zwieb & Brimacombe (1980); Stiege et al. (1986)

dimensional structure of the 16S rRNA. In experiments that used the TBE buffer system, some RNA molecules with apparently the same crosslinks are found in several adjacent fractions (Fig. 3). This may occur because the TBE gel system is not completely denaturing, so that molecules are spread out with an average mobility at the position of the observable band. This problem has been alleviated by the Bis-tris, borate, EDTA buffer system, which is more denaturing because it is used at a lower ionic strength. By combining this buffer system with the technique of varying the acrylamide:bisacrylamide ratio in the gels from 40:1 to 99:1, crosslink separation to single lane stops on primer extension gels has been achieved for most crosslinks.

A summary of the band identification is shown in Figure 5 on the gel electrophoresis pattern of a crosslinked sample that was separated with the BTBE buffer system. All, except three, of the bands that occur at the highest frequency as judged by the intensity of the gel electrophoresis pattern have had crosslinks assigned to them. The three bands visible in the gel electrophoresis pattern that have not been assigned crosslinks are one band above C54 × A535, and one above and one below U967 × C1400. In addition, there are approximately 12 orphan reverse transcription stops that occur in specific fractions and could be part of crosslinks, but for which we have not been able to establish partners. This may occur because some types of crosslinks are not detected with reverse transcriptase, or lay in parts of the reverse transcription patterns in which there are high backgrounds of nonspecific stopping and could not be observed. Some bands in the gel electrophoresis may arise from the different isomers of the same crosslinked RNA (Budowsky & Abdurashidova, 1989), and this may also contribute to an excess of bands over assigned crosslinks. One important site that we have not been able to assign as a crosslink with confidence involves position U793. RNA from the band below the one assigned as U967 × C1400 (Fig. 5) has a strong reverse transcription stop at position 794, indicating a crosslink at U793. A second reverse transcription stop at position 535 is found in this fraction and this would produce a loop of the expected size. However, the intensity of the stop at 535 is much less than expected, so it will need confirmation by another type of experiment.

The crosslinks listed in Table 1 are classified as either secondary or tertiary structure crosslinks based on whether or not the sites of crosslinking are in vicinity of one another in the secondary structure (see Fig. 6) according to Atmadja and Brimacombe (1985). The distinction is also useful because of their use in molecular modeling, as will be discussed in a following paragraph. Seven of our reported crosslinks correspond to crosslinked regions identified previously by Brimacombe and co-workers (Zwieb & Brimacombe, 1980; Atmadja & Brimacombe, 1985; Stiege et al., 1986, 1988; Doring et al., 1992). Because the sites had been determined by RNA fingerprinting, sequence intervals (usually 3–10 nt in length) had been reported for the sites of these crosslinks. The nucleotide positions that we have found for these crosslinks all fall within the intervals reported previously. Brimacombe and co-

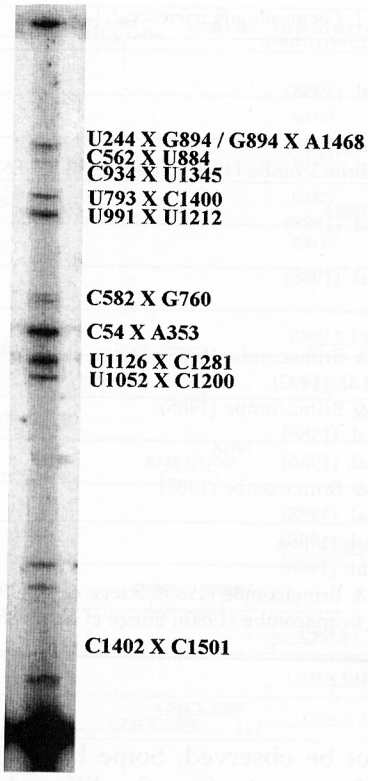

FIGURE 5. Assignment of crosslink identity to the gel electrophoresis banding pattern. Assignments shown here are a summary of the data in Figure 4 and similar results from additional experiments (data not shown). In this experiment, UV-crosslinked 16S rRNA was electrophoresed using the Bis-tris electrophoresis buffer system. In each case, associations are made between the sites of crosslinking in the RNA from each fraction and the strongest band within each interval, except that three types of molecules containing different crosslinks are assigned to the top-most band in the pattern.

workers also reported nine other UV-induced crosslinks (Table 1), many of which are short range (less than 100-nt loop size), and therefore may not be separated from the parent 16S rRNA under our gel conditions. We have not detected the presence of these in our experiments.

The exact determination of the sites for both the secondary-type and tertiary-type crosslinks is important for their use in the prediction of molecular models. Models for segments of 16S rRNA are being constructed (P. Babin & P. Wollenzien, unpubl.) using information for the chemical reactivity of the bases in the 30S subunit (Moazed et al., 1986) and other distance constraints with the program MC-SYM (Major et al., 1991); the UV crosslink information presented here can be incorporated into the models by including base-to-base distances in the description of the constraints. Of the eight secondary crosslinks, C582 × G760 is most straightforward to accommodate because it occurs between nucleotides on opposite strands of an interior loop. However, a new co-variance between C582 and C758 has been confirmed recently within this loop (R. Gutell, pers. comm.) and, this, with the known hyper-reactivity of A759 (Moazed et al., 1986) indicates unusual nucleotide geometries within this region. Other crosslinks (U562 × U884, C934 × U1345, U991 × U1212) bring together nucleotides that might otherwise be distant from one another in three-dimensional models for the corresponding regions. In general, these create some restrictions for the path of the single strands in which they are found, and limit the way in which adjacent base paired regions can be arranged, without affecting the geometry of the base pairs in the adjacent double-stranded regions. In three cases, crosslinks indicate interactions between nucleotides (C54 × A353, A441 × G494, and U1052 × C1200) that have to cross known base pairs. For the crosslinks C54 × A353 and U1052 × C1200, these interactions were incorporated into models only by allowing the base paired regions to form geometries that are not A type helices with normal Watson–Crick base pairs. The crosslink A441 × G494 occurs in an area of unusual geometry because two base pairs, U438·A496 and C440·G497, require the strands to be arranged parallel for a short interval. The crosslink C1402 × C1501 must also be in an area of unusual geometry because these nucleotides are opposite and adjacent in neighboring base pairs and normally would not be expected to be in crosslinking distance if they belonged to an A-form helix. Details of these structures will be presented elsewhere (P. Babin & P. Wollenzien, in prep.).

Because the tertiary structure crosslinks join sites distant in the secondary structure, they provide valuable information about the three-dimensional folding of the 16S rRNA. However, there is no supporting information for specific interactions between the crosslinked sites, and it is difficult to know if there is any stable contact between them or if they are simply in the vicinity of one another, covalent crosslinks forming during transient contacts. In this set of crosslinks, two (U244 × G894 and G894 × A1468) share a common nucleotide; this probably indicates a dynamic area of the subunit, although a three-way interaction of the involved nucleotides cannot be excluded yet. The tertiary structure crosslinks U244 × G894 and U1126 × C1281, which join regions within RNA domains I+II and III, respectively, have been known for some time at lower resolution and they have been included in three-dimensional models in the last three years (Malhotra & Harvey, 1994; Brimacombe, 1995). The three new crosslinks reported here provide some new information about folding within domain III and between domains II and III and the decoding region in the 16S rRNA. The crosslink C967 × C1400 indicates a short distance between the end loop of base paired region 31 and nt C1400. The crosslink G894 × A1468 connects G894 to a site in the middle of the long penultimate

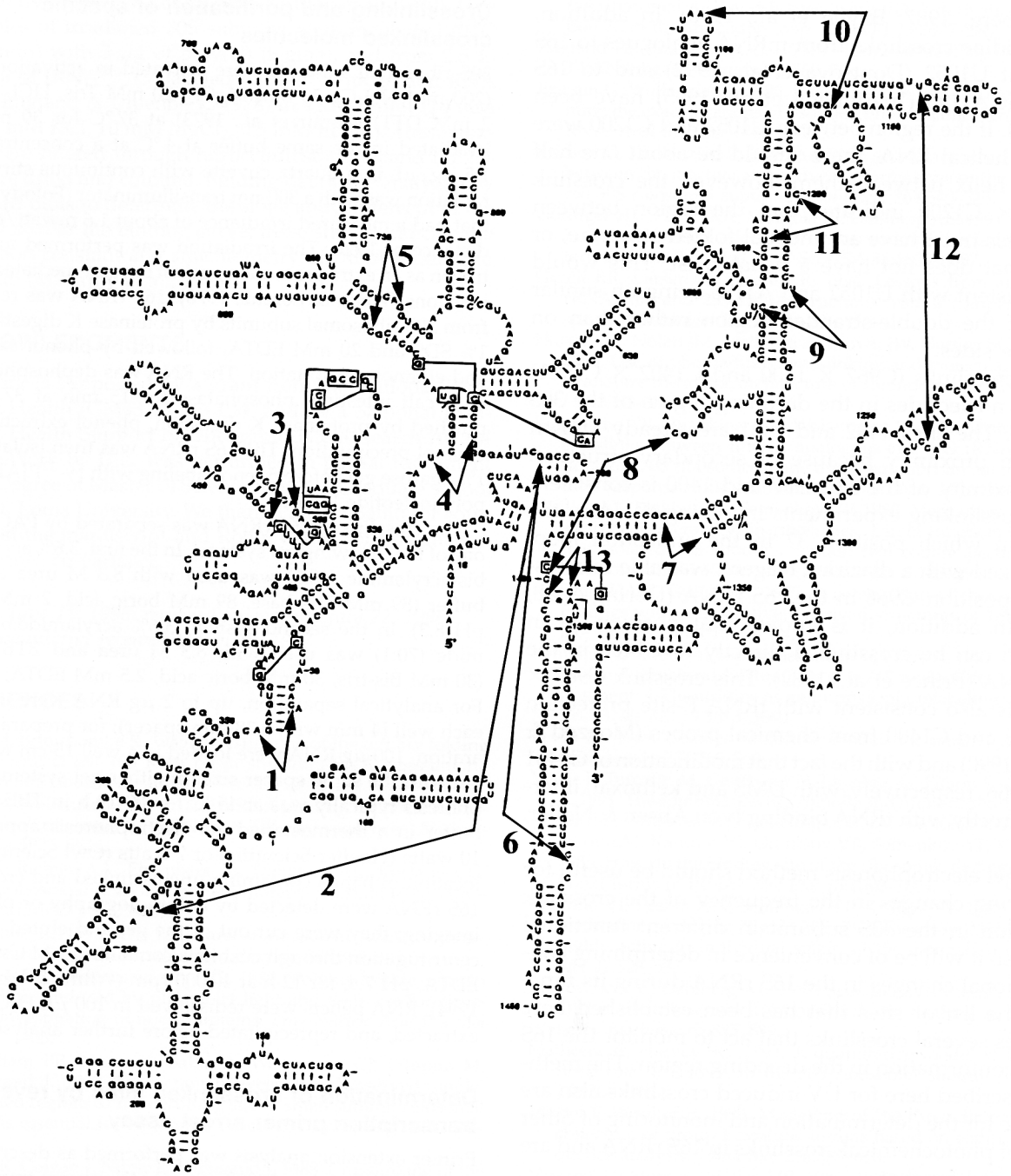

FIGURE 6. Summary of crosslinking sites on the *E. coli* 16S rRNA secondary structure. Arrows connect the nucleotides involved in 11 crosslinks determined in these experiments (see Table 1, which uses the same numbering for the crosslinks and crosslink positions). This version of the secondary structure is reproduced from Gutell et al. (1994), with permission.

duplex region (nt 1399–1504). The position of G894 is constrained by its location in the secondary structure and its crosslink with A244, so this crosslink helps to indicate the position and rotation of the helix containing A1468. This is important because it will help determine how the decoding region is arranged in the 30S subunit.

The function of several of the regions around these crosslinking sites is important. The crosslink U1052 × A1200 is of functional interest because deletion of C1054, and mutations at additional sites in the region, determine read-through of UGA termination codons (Murgola et al., 1988; Goringer et al., 1991; Moine & Dahlberg, 1994) and other effects, including read-through of the other termination codons and altered fidelity (Prescott et al., 1991; Prescott & Kornau, 1992; Triman, 1995). Mutations in this region also confer spectinomycin resistance (Sigmund et al., 1984; Makowsky

& Dahlberg, 1987; Bilgen et al., 1990). In addition, 4-thiouridine crosslinks from mRNA analogues to 16S rRNA nt U1052 (Dontsova et al., 1992) and to 16S rRNA nt A1196 (Juzumiene et al., 1995) have been reported. If the region between U1052 and C1200 were A-form helical RNA, there should be about one half turn of helix between them; however, the crosslink U1052 × C1200 indicates that the region between these sites must have an unusual folded structure, or bend, that does not have a usual twist. This would be consistent with U1052 and A1196 being on similar sides of the double-stranded region rather than on opposite sides.

Two crosslinks (C967 × 1400 and C1402 × C1501) involve nucleotides in the decoding region of the 30S subunit. The sites 1402 and 1501 are already known to be in proximity because of secondary structure. The proximity of the sites 967 and 1400 is consistent with crosslinking experiments involving tRNA in the P site in which position 32 in the anticodon loop, derivatized with a diazirine reagent, was able to crosslink to position G966 in the 16S rRNA (Doring et al., 1994). In addition, it is known that position 34 in $tRNA^{Val}$ can be crosslinked directly to C1400 in the 16S rRNA (Prince et al., 1982). This crosslink C967 × C1400 is also consistent with tRNA P-site protection of G966 and C1400 from chemical probes (Moazed & Noller, 1990) and with the fact that modification of G1401 and G966, respectively, with DMS and kethoxal, interferes directly with tRNA binding (von Ahsen & Noller, 1995).

The gel electrophoresis method should be useful for measuring changes in the frequency of the crosslink formation in the 30S subunit in different functional states, so it will be of convenience in determining conformational changes in the 16S rRNA during its function. The list of sites that has been established here includes several crosslinks that act to monitor the 16S rRNA conformation in the decoding region. The methods described here for UV-induced crosslinks also are suitable for the determination and monitoring of other types of photochemical crosslinks in 16S rRNA and are being used for that.

MATERIALS AND METHODS

Preparation of ribosomes

E. coli 70S ribosomes and ribosomal subunits were prepared according to Makhno et al. (1988), except that washed 70S ribosomes rather than washed, purified tight couple 70S ribosomes were used for the isolation of ribosomal subunits. Frozen *E. coli* MRE 600 (1/2 log) cells (Cell Culture Fermentation Facility, University of Alabama, Birmingham) were usually used, and these gave the same results as cells prepared in small scale and used immediately.

Crosslinking and purification of specific crosslinked molecules

30S ribosomal subunits were activated in activation buffer (200 mM NH_4Cl, 20 mM $MgCl_2$, 20 mM Tris, HCl, pH 7.5, 2 mM DTT) (Zamir et al., 1973) at 37 °C for 30 min and irradiated in the same buffer at 4 °C at a concentration of 1.5 $\mu g/\mu L$ in a quartz cuvette with continuous stirring. Irradiation was with a 300-nm transilluminator (Fotodyne, Inc.) that had a measured irradiance of about 1.6 mwatt/cm^2 at a distance of 1 cm. The irradiation was performed under nitrogen as an extra precaution against oxygen-mediated photoreactions (Webb & Lorenz, 1970). 16S rRNA was recovered from 30S ribosomal subunits by proteinase K digestion with 1% SDS and 20 mM EDTA, followed by phenol extraction and ethanol precipitation. The RNA was dephosphorylated with calf intestinal phosphatase for 15 min at 37 °C, and purified by proteinase K digestion, phenol extraction, and ethanol precipitation. The 16S rRNA was then isolated on a 1% agarose gel before 5′ end-labeling with [γ-^{32}P]ATP by T4 polynucleotide kinase.

The crosslinked 16S rRNA was separated by PAGE using one of the following gel systems. In the first, 3.6% acrylamide: bis-acrylamide (40:1) was used with 8.3 M urea and TBE buffer (89 mM Tris base, 89 mM boric acid, 2 mM EDTA, pH 8.3). In the second system, 3.6% acrylamide:bisacrylamide (70:1) was used with 8.3 M urea and BTBE buffer (30 mM Bis-tris, 30 mM boric acid, 2.5 mM EDTA, pH 6.8). For analytical separation, up to 2 μg RNA were loaded in each well (4 mm with 0.38-mm spacer); for preparative separation, 100 μg RNA were loaded in a well 15-cm wide on a gel with the same spacer size. In either gel system, electrophoresis typically was at 45 °C for 16–19 h in TBE or BTBE buffer in a thermostatted gel electrophoresis apparatus at 10 watts (Hoeffer Scientific) or 7 watts (Owl Scientific). The location of bands containing uncrosslinked and crosslinked 16S rRNA were detected by autoradiography or phosphorimaging; they were cut out of the gel and eluted by ultracentrifugation through cushions containing 2 M CsCl, 0.2 M EDTA, pH 7.4, for 12 h at 40,000 rpm (Wilms & Wollenzien, 1994). RNA pellets were redissolved in 100 μL H_2O, phenol extracted, and reprecipitated before further analysis.

Determination of crosslinked sites by reverse transcription primer arrest assay

Primer extension analysis was performed as described previously (Wollenzien, 1988) using AMV reverse transcriptase (Type 007, Life Sciences, Inc.). Bases involved in UV-induced crosslinks are identified by the presence of an increased stop in the reverse transcription pattern; the stop occurs one nucleotide in the 3′ direction of the crosslinked base (Denman et al., 1988; Cunningham et al., 1992). Ten DNA primers complementary to regions throughout the 16S rRNA were used (Bhangu & Wollenzien, 1992) to allow reading of the 16S rRNA, except for the 3′-terminal 40 nt. Reverse transcription reactions were electrophoresed on 8% acrylamide: bis-acrylamide (19:1), 8.3 M urea in TBE buffer.

tRNA binding assay

Experiments were performed to test the ability of UV-irradiated 30S subunits to bind $tRNA^{Phe}$ in the presence of

poly (U) (Nirenberg & Leder, 1964; Kirillov et al., 1980). Five picomoles of irradiated 30S subunits were incubated (0 °C for 60 min) with 5 μg of poly(U) (Sigma), and from 2.5 to 25 pmol of $tRNA^{Phe}$ (3′ labeled with [5′^{32}P]pCp) and RNA ligase (England & Uhlenbeck, 1978) in TKM buffer (10 mM Tris, 50 mM KCl, 10 mM $MgCl_2$, 0.5 mM EDTA). These mixtures were filtered through nitrocellulose filters and the filters were dried and counted. Binding data were analyzed by Scatchard plots to determine the slope and x intercept of the steepest part of the binding curve; these should indicate the association constant and stoichiometry of tRNA binding to the P site (Makarov et al., 1985).

ACKNOWLEDGMENTS

This work is supported by a grant from the National Institutes of Health (GM43237) to P.W. and by a National Institutes of Health Support of Undergraduate Research Award to C.W. Work by D.Z. was performed in partial fulfillment for the Degree of Master of Science from the Graduate School of the St. Louis University. We thank Patricia Babin for comments on the manuscript and Robin Gutell for information on sequence co-variance.

Received June 14, 1996; returned for revision July 22, 1996; revised manuscript received March 19, 1997

REFERENCES

Atmadja J, Brimacombe R. 1985. Investigation of the tertiary folding of *Escherichia coli* 16S RNA by in situ intra-RNA cross-linking within 30S ribosomal subunits. *Nucleic Acids Res 13*:6919–6937.

Bhangu R, Wollenzien P. 1992. The mRNA binding rack in the *Escherichia coli* ribosome for mRNAs of different sequences. *Biochemistry 31*:5937–5944.

Bilgen N, Richter AA, Ehrenberg M, Dahlberg AE, Kurland CG. 1990. Ribosomal RNA and protein mutants resistant to spectinomycin. *EMBO J 9*:735–739.

Brimacombe R. 1995. The structure of ribosomal RNA: A three-dimensional jigsaw puzzle. *Eur J Biochem 230*:365–383.

Budowsky EI, Abdurashidova GG. 1989. Polynucleotide-protein cross-links induced by ultraviolet light and their use for structural investigation of nucleoproteins. *Prog Nucleic Acid Res Mol Biol 37*:1–65.

Cunningham PR, Nurse K, Bakin A, Weitzmann CJ, Pflumm M, Ofengand J. 1992. Interaction between two conserved single-stranded regions at the decoding site of small subunit ribosomal RNA is essential for ribosomes function. *Biochemistry 31*:12012–12022.

Denman R, Colgan J, Nurse K, Ofengand J. 1988. Crosslinking of the anticodon of P site bound tRNA to C-1400 of *E. coli* 16S rRNA does not require the participation of the 50S subunit. *Nucleic Acids Res 16*:165–178.

Denman R, Negre D, Cunningham PR, Nurse K, Colgan J, Weitzmann C, Ofengand J. 1989. Effect of point mutations in the decoding site (C1400) region of 16S ribosomal RNA on the ability of ribosomes to carry out individual steps of protein synthesis. *Biochemistry 28*:1012–1019.

Dontsova O, Dokudovskaya S, Kopylov A, Bogdonov A, Rinke-Appel J, Junke N, Brimacombe R. 1992. Three widely separated positions in the 16S RNA lie in or close to the ribosomal decoding region; a site directed cross-linking study with mRNA analogues. *EMBO J 11*:3105–3116.

Doring T, Greuer B, Brimacombe R. 1992. The topography of the 3′-terminal region of *Escherichia coli* 16S ribosomal RNA; an intra-RNA cross-linking study. *Nucleic Acids Res 20*:1593–1597.

Doring T, Mitchell P, Osswald M, Bochkariov D, Brimacombe R. 1994. The decoding region of 16S RNA; a cross-linking study of the ribosomal A, P and E sites using tRNA derivatized at position 32 in the anticodon loop. *EMBO J 13*:2677–2685.

England TE, Uhlenbeck OC. 1978. 3′-Terminal labelling of RNA with T4 RNA ligase. *Nature 275*:560–561.

Ericson G, Wollenzien P. 1986. Use of reverse transcription to determine the exact locations of psoralen photochemical cross-links in RNA. *Anal Biochem 174*:215–223.

Ericson G, Wollenzien P. 1988. An RNA secondary structure switch between the inactive and active conformations of the *Escherichia coli* 30S ribosomal subunit. *J Biol Chem 264*:540–545.

Goringer HU, Hijazi KA, Murgola EJ, Dahlberg AE. 1991. Mutations in 16S rRNA that affect UGA (stop codon)-directed translation termination. *Proc Natl Acad Sci USA 88*:6603–6607.

Gutell RR, Larsen N, Woese CR. 1994. Lessons from an evolving rRNA: 16S and 23S rRNA structures from a comparative perspective. *Microbiol Rev 58*:10–26.

Harris ME, Nolan JM, Malhotra A, Brown JW, Harvey SC, Pace NR. 1994. Use of photoaffinity crosslinking and molecular modeling to analyze the global architecture of ribonuclease P RNA. *EMBO J 13*:3953–3963.

Juzumiene DI, Shapkina TG, Wollenzien P. 1995. Distribution of crosslinks between mRNA analogues and 16S rRNA in *Escherichia coli* 70S ribosomes made under equilibrium conditions and their response to tRNA binding. *J Biol Chem 270*:12794–12800.

Kirillov SV, Makhno VI, Semenkov YP. 1980. Mechanism of codon-anticodon interaction in ribosomes. Direct functional evidence that isolated 30S subunits contain two codon-specific binding sites for transfer RNA. *Nucleic Acids Res 8*:183–196.

Konings DAM, Gutell RR. 1995. A comparison of thermodynamic foldings with comparatively derived structures of 16S and 16S-like rRNAs. *RNA 1*:559–574.

Lemaigre-Dubreuil Y, Expert-Bezancon A, Favre A. 1991. Conformation and structural fluctuations of a 218 nucleotides long rRNA fragment: 4-Thiouridine as an intrinsic photolabeling probe. *Nucleic Acids Res 19*:3653–3660.

Levitt M. 1969. Detailed molecular models for transfer ribonucleic acid. *Nature 224*:759–763.

Major F, Turcotte M, Gautheret D, Lapalme G, Fillion E, Cedergren R. 1991. The combination of symbolic and numerical computation for three-dimensional modeling of RNA. *Science 253*:1255–1260.

Makarov EM, Katunin VI, Odintsov VB, Semenkov YP, Kirillov SV. 1985. How do the binding site of the ribosomes distinguish functional forms of tRNA? *Mol Biol 18*:1090–1094.

Makhno VI, Peshin NN, Semenkov YP, Kirillov SV. 1988. Modified method of producing "tight" 70S ribosomes from *Escherichia coli*, highly active in individual stages of the elongation cycle. *Mol Biol 22*:528–537.

Makowsky PC, Dahlberg AE. 1987. Spectinomycin resistance at site 1192 in 16S ribosomal RNA of *E. coli*: An analysis of three mutants. *Biochimie 69*:885–889.

Malhotra A, Harvey SC. 1994. A quantitative model of the *Escherichia coli* 16 S RNA in the 30S ribosomal subunit. *J Mol Biol 240*:308–340.

Michel F, Westhof E. 1990. Modelling of the three-dimensional architecture of group I catalytic introns based on comparative sequence analysis. *J Mol Biol 216*:585–610.

Moazed D, Stern S, Noller HF. 1986. Rapid chemical probing of conformation in 16S ribosomal RNA and 30S ribosomal subunits using primer extension. *J Mol Biol 187*:399–416.

Moazed D, Noller HF. 1990. Binding of tRNA to the ribosomal A and P sites protects two distinct sets of nucleotides in 16S rRNA. *J Mol Biol 211*:135–145.

Moine H, Dahlberg AE. 1994. Mutations in helix 34 of *Escherichia coli* 16S ribosomal RNA have multiple effects on ribosome function and synthesis. *J Mol Biol 243*:402–412.

Murgola EJ, Hijazi KA, Goringer HU, Dahlberg AE. 1988. Mutant 16S ribosomal RNA: A codon-specific translational suppressor. *Proc Natl Acad Sci USA 85*:4162–4165.

Nirenberg M, Leder P. 1964. RNA codewords and protein synthesis. *Science 145*:1399–1407.

Peattie DA. 1979. Direct chemical method for sequencing RNA. *Proc Natl Acad Sci USA 76*:1760–1764.

Prescott C, Krabben L, Nierhaus K. 1991. Ribosomes containing the C1054-deletion mutation in *E. coli* 16S rRNA act as suppressor at all three nonsense codons. *Nucleic Acids Res 19*:5281–5283.

Prescott CD, Kornau HC. 1992. Mutations in *E. coli* 16S rRNA that enhance and decrease the activity of a suppressor tRNA. *Nucleic Acids Res 20*:1567–1571.

Prince J, Taylor BH, Thurlow DL, Ofengand J, Zimmermann RA. 1982. Covalent crosslinking of $tRNA_1^{Val}$ to 16S RNA at the ribosomal P site: Identification of crosslinked residues. *Proc Natl Acad Sci USA 79*:5450–5454.

Quigley G, Rich A. 1976. Structural domains of transfer RNA molecules. *Science 194*:796–806.

Rinke-Appel J, Junke N, Stade K, Junke N, Brimacombe R. 1991. The path of mRNA through the *Escherichia coli* ribosome; site-directed cross-linking of mRNA analogues carrying a photoreactive label at various points 3′ to the decoding site. *EMBO J 10*:2195–2202.

Sigmund CD, Ettayebi M, Morgan EA. 1984. Antibiotic resistance mutations in 16S and 23S ribosomal RNA genes of *Escherichia coli*. *Nucleic Acids Res 12*:4653–4663.

Stiege W, Atmadja J, Zobawa M, Brimacombe R. 1986. Investigation of the tertiary folding of *Escherichia coli* ribosomal RNA by intra-RNA cross-linking in vivo. *J Mol Biol 191*:135–138.

Stiege W, Kosack M, Stade K, Brimacombe R. 1988. Intra-RNA cross-linking in *Escherichia coli* 30S ribosomal subunits: Selective isolation of cross-linked products by hybridization to specific cDNA fragments. *Nucleic Acids Res 16*:4315–4329.

Sussman JL, Kim SH. 1976. Three-dimensional structure of a transfer RNA in two crystal forms. *Science 192*:853–858.

Teare J, Wollenzien P. 1989. Structures of human and rabbit beta globin messenger RNA precursors in solution. *Biochemistry 28*: 6208–6219.

Teare J, Wollenzien P. 1990. The structure of a pre-mRNA molecule in solution determined with a site-directed cross-linking reagent. *Nucleic Acids Res 18*:855–864.

Thompson JF, Hearst JE. 1983. Structure of *E. coli* 16S RNA elucidated by psoralen crosslinking. *Cell 32*:1355–1365.

Triman KL. 1995. Mutational analysis of 16S ribosomal RNA structure and function in *Escherichia coli*. *Adv Genetics 33*:1–39.

von Ahsen U, Noller HF. 1995. Identification of bases in 16S rRNA essential for tRNA binding at the 30S ribosomal P site. *Science 267*:234–237.

Webb RB, Lorenz JR. 1970. Oxygen dependence and repair of lethal effects of near ultraviolet and visible light. *Photochem Photobiol 12*:283–289.

Weeks KM, Cech TR. 1995. Protein facilitation of group I intron splicing by assembly of the catalytic core and the 5′ splice site. *Cell 82*:221–230.

Wilms C, Wollenzien P. 1994. Purification of RNA from polyacrylamide gels by ultracentrifugation. *Anal Biochem 221*:204–205.

Wollenzien P. 1988. Isolation and identification of RNA cross-links. *Methods Enzymol 164*:319–329.

Zamir A, Miskin R, Vogel A, Elson D. 1973. The inactivation and reactivation of *Escherichia coli* ribosomes. *Methods Enzymol 30*:406–426.

Zwieb C, Brimacombe R. 1979. RNA–protein cross-linking in *Escherichia coli* 30S ribosomal subunits: Precise localisation of the nucleotide in 16S RNA which is coupled to protein S7 by ultraviolet irradiation. *Nucleic Acids Res 6*:1775–1790.

Zwieb C, Brimacombe R. 1980. Localisation of a series of intra-RNA cross-links in 16S RNA, induced by ultraviolet irradiation of *Escherichia coli* 30S ribosomal subunits. *Nucleic Acids Res 8*:2397–2411.

Zwieb C, Ross A, Rinke J, Meinke M, Brimacombe R. 1978. Evidence for RNA–RNA cross-link formation in *Escherichia coli* ribosomes. *Nucleic Acids Res 5*:2705–2720.